Supporting Information of

Realizing Multiferroics in α-Ga_2S_3 via Hole-doping: A First-Principles Study

Junwen Zhong[1,2], Peng Wu[1], Zengying Ma[2], Xueqian Xia[2,3], Bowen Song[1], Yanghong Yu[3], Sufan Wang[1,3,], Yucheng Huang[1,2]**

[1]College of Chemistry and Material Science, Key Laboratory of Functional Molecular Solids, Ministry of Education, Anhui Normal University, Wuhu 241000, China

[2]Anhui Key Laboratory of Molecule-Based Materials, Anhui Carbon Neutrality Engineering Center, Anhui Normal University, Wuhu 241000, China

[3]Key Laboratory of Electrochemical Clean Energy of Anhui Higher Education Institutes, Anhui Provincial Engineering Laboratory of New-Energy Vehicle Battery Energy-Storage Materials, Anhui Normal University, Wuhu 241000, China

E-mail: sfwang@mail.ahnu.edu.cn; huangyc@mail.ahnu.edu.cn

NOTE 1: Test of functionals

The choice of functionals, i.e., PBE, HSE06, PBE0, and B3LYP, were carefully tested by comparing the calculated lattice parameters, band gaps, and the formation energies of V_{Ga} with the available theoretical results at the same level of theory in literatures. As listed in Table S1, the lattice parameters are insensitive to the functionals while the band gap calculated at the level of HSE06 and B3LYP is close to each other. On the other hand, for the formation energies, the PBE level gives the same results to those of HSE06, which is lower in ~ 0.2 eV to those of B3LYP. Thus, in our work, we used the PBE functional to optimize the geometries and obtain the total energy while adopted the HSE06 functional to calculate the electronic properties.

TABLE S1. The lattice constant a, band gap E_g of the pristine α-Ga_2S_3, and formation energy E_f of V_{Ga} under Ga-rich and S-rich conditions are calculated by PBE, HSE06, PBE0, and B3LYP functionals.

	Pristine α-Ga_2S_3 unit cell		Intrinsic defect gallium vacancy	
	a	E_g	E_f (Ga-rich)	E_f (S-rich)
	Å	eV	eV	
PBE	3.62	1.74	3.47	2.52
HSE06	3.62	2.68	3.47	2.52
PBE0	3.62	3.42	4.24	3.29
B3LYP	3.64	3.07	3.70	2.75
Ref.[1]	3.59^{PBE}	1.79^{PBE}		
Ref.[2]		2.71^{HSE06}		

NOTE 2: Calculation method of ferroelectrics

The in-plane and out-of-plane electric polarizations were calculated by Berry Phase method[3] based on the optimized geometrics, and the total polarization can be expressed as the sum of ion and electron components $\Delta P_{tot} = \Delta P_{ion} + \Delta P_{elec}$. The SSNEB method (Solid State Nudged Elastic Band method)[4] was applied to calculate the energy barrier of kinetic process. In this method, the total energy was expressed

by Landau-Ginzburg expansion[5]:

$$E = \sum_i \frac{A}{2} p_i^2 + \frac{B}{4} p_i^4 + \frac{C}{6} p_i^6 + \frac{D}{2} \sum_{<i,j>} (p_i - p_j)^2 \quad \text{(S-1)}$$

Here, P_i is the polarization of each unit cell, A, B, C, D are Landau coefficients, and i, j denotes the nearest neighbors. The first three terms of the equation describe an anharmonic double-well potential, and the last term captures the dipole-dipole coupling between the nearest adjacent neighbors, which can be approximated by using the mean field theory and assuming that only the nearest neighbor interaction exists.

NOTE 3: Calculation method of intrinsic defects

We used defect formation energy to estimate the stability of different defects. The formation energy of the charged defect $\Delta H_{D,q}$[6,7,8] is defined as:

$$\Delta H_{D,q} = E_{D,q} - E_H - \sum_\alpha n_\alpha \mu_\alpha + q(E_F + E_V + \Delta V) \quad \text{(S-2)}$$

Here, $E_{D,q}$ represents the total energy of the supercell of the defect when the charge state is q, and E_H is the total energy of the perfect supercell with the same size. n_α (α represents Ga or S atoms) refers to the number of atoms taken from the supercell model ($n_\alpha < 0$) or added ($n_\alpha > 0$) to form defects in the supercell, and μ_α is the chemical potential of the atom. q represents the number of electrons transferred from the defect energy level to the top of the valence band (acceptor defect, $q < 0$) or the bottom of the conduction band (donor defect, $q > 0$)[9]. E_F is the Fermi energy level relative to the VBM energy position in the perfect α-Ga_2S_3 supercell, and the eigenvalues in different supercells should be aligned with the same reference energy level (the valence band top of the perfect material). ΔV is the potential correction, which is used to align the electrostatic potential between the pure crystal cell and the defect system of the same size. The specific calculation is the defect electrification correction divided by the real part of optical absorption coefficient of the perfect α-Ga_2S_3 supercell.

For the calculation of formation energies and thermodynamic transition energy levels, we simulated two different growth conditions, i.e., rich gallium (Ga-rich) and

rich sulfur (S-rich). To avoid the formation of gallium or sulfur bulks, the chemical potential of gallium or sulfur must be less than their respective bulk values[9,10]. As shown in Fig. S1, the upper limits of the chemical potential of Ga and S bulk phases are shown by black vertical lines and parallel lines, respectively. In order to achieve uniform growth of α-Ga_2S_3 crystals, the chemical potentials of Ga and S atoms must be consistent with the following constraints:

$$\mu_{Ga_2S_3} = 2\mu_{Ga} + 3\mu_S \quad \text{(S-3)}$$

$\mu_{Ga_2S_3}$represents the chemical potential of α-Ga_2S_3 monolayer. The above formula gives the equilibrium growth conditions: if the sum of μ_{Ga} and μ_S is greater than $\mu_{Ga_2S_3}$, the balance will move to the left, resulting in non-uniform growth of α-Ga_2S_3 crystals; if the sum of the two terms on the right is less than $\mu_{Ga_2S_3}$, α-Ga_2S_3 will decompose. The calculated formation energy of α-Ga_2S_3 is -22.40 eV per molecular formula, which is expressed by the blue solid line.

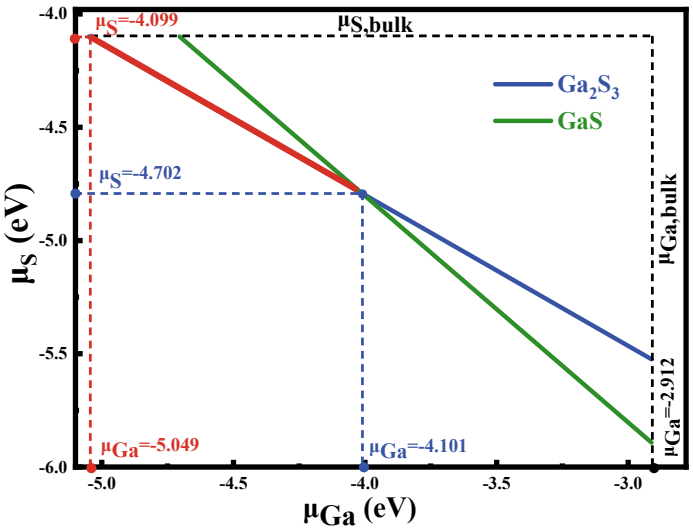

Thermodynamic growth condition of α-Ga_2S_3 crystal.

The black horizontal and vertical dashed lines represent the upper limits of sulfur and gallium, which are determined by the natural phases of sulfur and gallium. The solid blue and green lines give the conditions for the balanced growth of α-Ga_2S_3 and GaS. The allowable range of conditions for balanced growth of α-Ga_2S_3 crystals is marked with red thick solid lines.

In addition, for the α-Ga_2S_3, another phase of GaS may coexist in the system. Compared with α-Ga_2S_3, the gallium/sulfur ratio of GaS is higher, indicating that the effective growth of GaS phase tends to be in Ga-rich condition. To restrain the formation of this unwanted phase, the growth conditions must be limited below the upper limit of μ_{Ga}. Under the thermodynamic equilibrium of GaS, the chemical potentials of gallium and sulfur atoms must satisfy the following constraint conditions:

$$\mu_{GaS} = \mu_{Ga} + \mu_S \tag{S-4}$$

The calculated formation energy of GaS is -8.803 eV per molecular formula, and the solid green line in Fig. S1 marks the growth conditions of GaS. It can be seen from the figure that the lines corresponding to formulas (S-3) and (S-4) intersect at μ_{Ga} = -4.101 eV (μ_S = -4.702 eV). With the increase of μ_{Ga}, the formation energy of α-Ga_2S_3 is higher than that of GaS, which means that the GaS phase will take the place of α-Ga_2S_3 in the Ga-rich condition. Therefore, we believe that μ_{Ga}= -4.101eV is the real upper limit of α-Ga_2S_3 growth. The red solid line clearly marks the chemical potential range in which α-Ga_2S_3 can grow in equilibrium.

The transition energy level ε(q/q') of a defect refers to the Fermi energy level when the defect changes from the charged state of q to the charged state of q', and the defect formation energy corresponding to the two different valence states is equal. It can be seen from the formula (S-2) that the formation energy of neutral defects does not change with the position of the Fermi level, but for charged defects, the formation energy changes. The conversion energy level is calculated as[10,11]:

$$\varepsilon(q/q') = \frac{\Delta H_{D,q} - \Delta H_{D,q'}}{q - q'} \tag{S-5}$$

Except for the neutral state, the valence states of all the intrinsic defects considered in this paper range from -2 to +3. Since not all the valence states are stable for these intrinsic defects, only the most stable valence states were discussed.

NOTE 4: Test of supercell size

For the pristine Ga_2S_3 monolayer, constructing the size of 3 × 3 × 1 supercell is a conventional choice. For the defective Ga_2S_3 monolayer, the sizes of 2 × 2 × 1, 3 × 3 × 1, 4 × 4 × 1 and 5 × 5 × 1 were tested using the calculated formation energies V_{Ga} as the convergence criterion. As tabulated in Table S2, the results of 3 × 3 × 1 supercell deviate slightly to those of 5 × 5 × 1 one. Taking into consideration both computational economy and accuracy, the size of 3 × 3 × 1 supercell was chosen in our investigation.

TABLE S2. Test of supercell size using the calculated formation energies V_{Ga} as the convergence criterion.

Supercell size	Number of atoms	E_f (Ga-rich)	E_f (S-rich)
		eV	
2 × 2 × 1	19	3.65	2.71
3 × 3 × 1	44	3.47	2.52
4 × 4 × 1	79	3.42	2.47
5 × 5 × 1	124	3.40	2.45

NOTE 5: Validation of FM for the V_{Ga}

To validate the FM, we double the size of the supercell by placing two 45-atom units side by side, *i.e.*, two V_{Ga} centers are placed equidistantly in the 90-atom supercell. The distance between two adjacent V_{Ga} is 10.88 Å. Depending on the initial spin alignments, self-consistent calculations give two stable spin configurations: one is ferromagnetic (FM), the other is antiferromagnetic (AFM). The energetic difference between the two phases, $\Delta E = E_{AFM} - E_{FM}$, is used to evaluate the magnetic interactions. For one hand, the magnetic moment with two V_{Ga} defects is 4.66 μ_B, which is slightly less than twice of a single V_{Ga} (2.39 μ_B). On the other hand, the energy difference ΔE is +25 meV, which proves that the coupling between the two defects is a kind of FM. The spin density of one V_{Ga} in 45-atom and two V_{Ga} in 90-atom supercell are depicted in the following figure, which also clearly supports the FM coupling for the V_{Ga}.

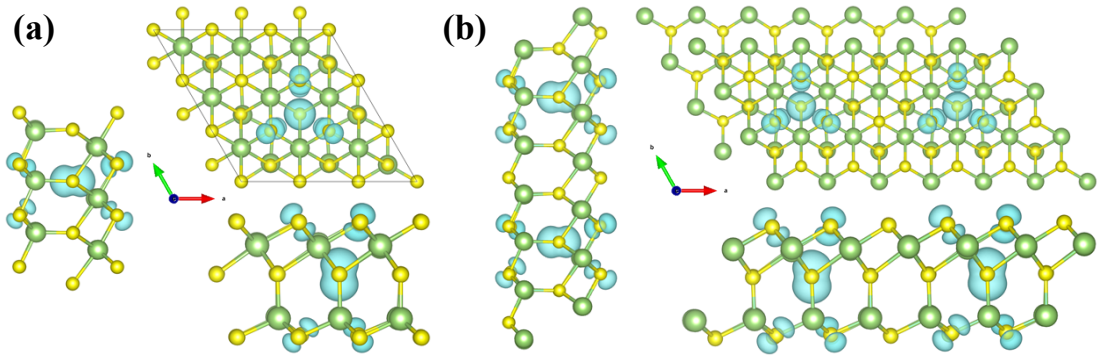

(a) Spin density of V_{Ga} in a 3 × 3 × 1 supercell; (b) Spin density of V_{Ga} in a 6 × 3 × 1 supercell.

Supporting Figures:

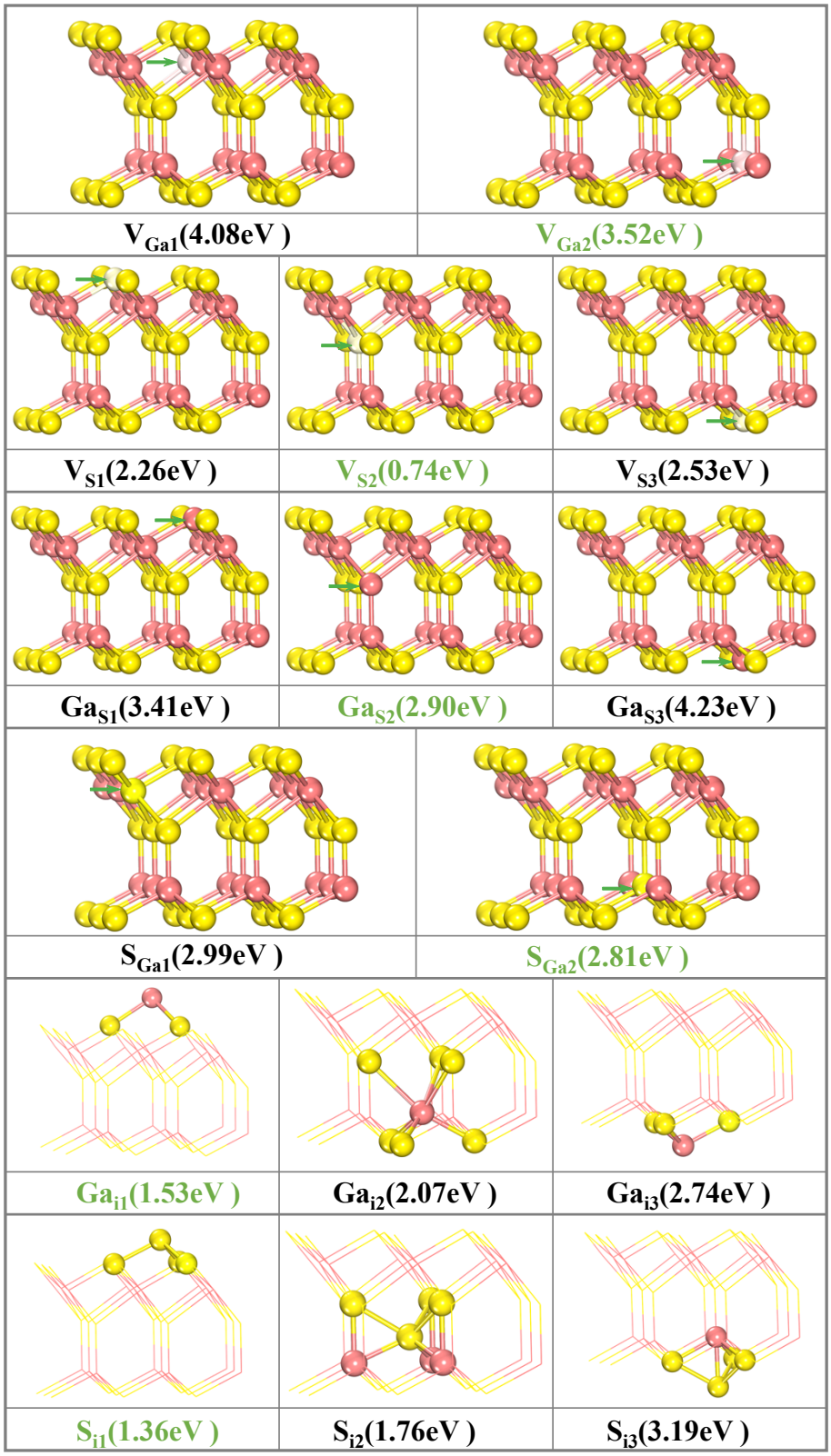

FIG. S1 Various possible configurations of defects. The numbers are the corresponding formation energies of each considered structure under the Ga-rich condition, in which the one marked with green is the most stable configuration.

FIG. S2 Variations of the temperature and total energy vs time for AIMD simulations of pristine α-Ga_2S_3 monolayer and V_{Ga}. The simulations last 5 ps with a time step of 1.0 fs, and the temperature was set to 300 K. Insets are the side views of snapshots at 5 ps.

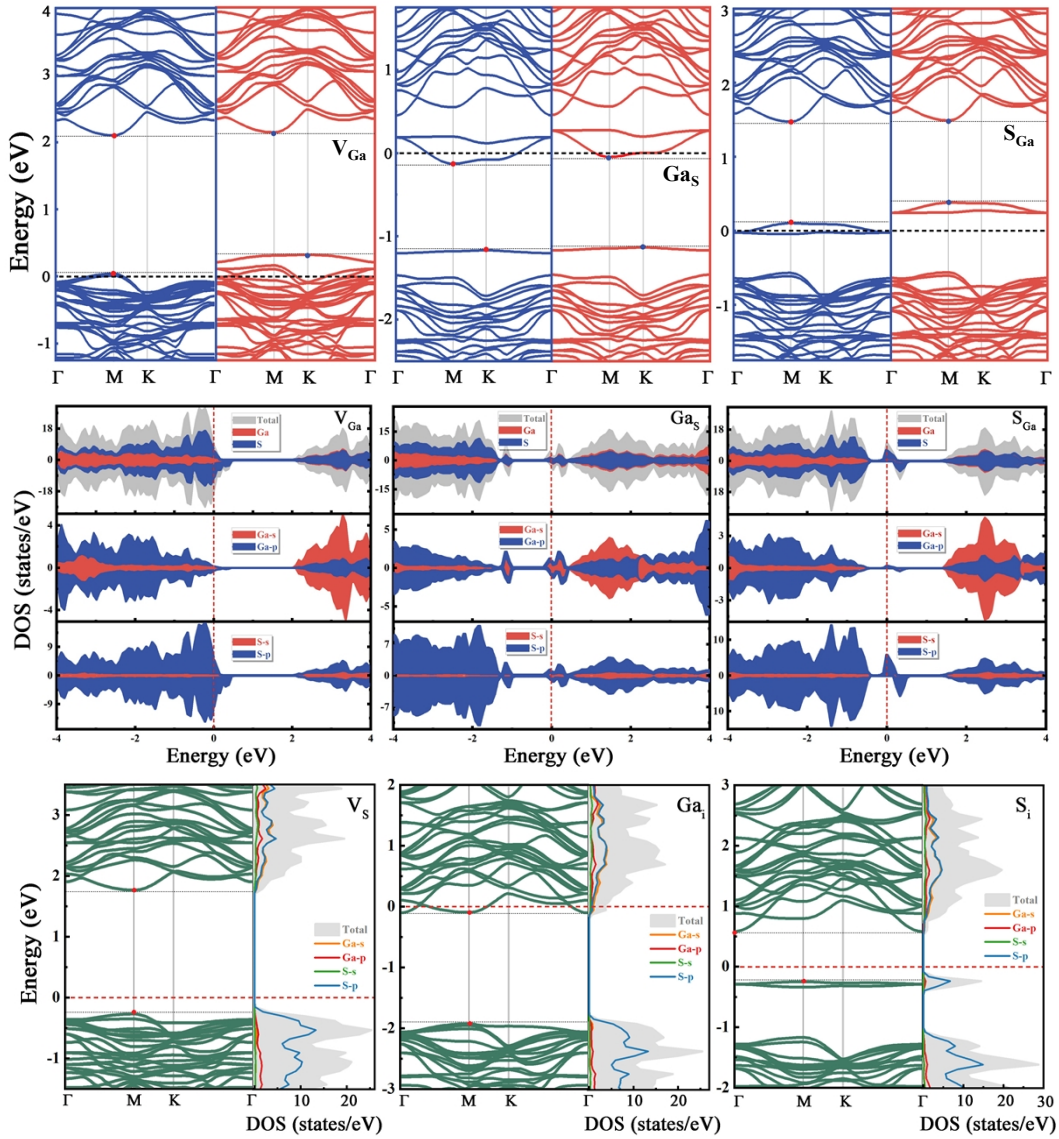

FIG. S3 Band Structures and density of states (DOS) of α-Ga_2S_3 with various intrinsic defects.

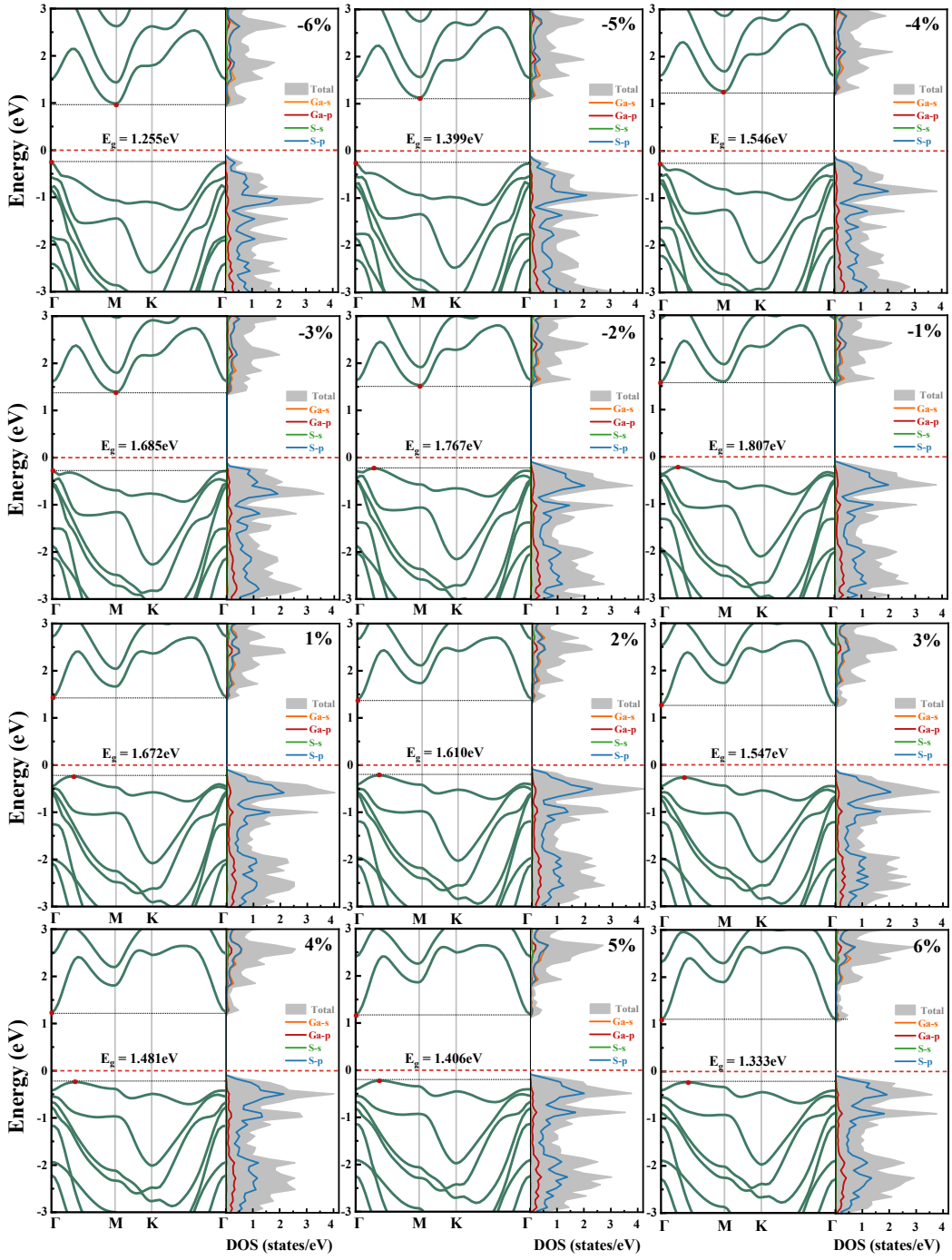

FIG. S4 Band structures and DOS of α-Ga_2S_3 under uniaxial strain.

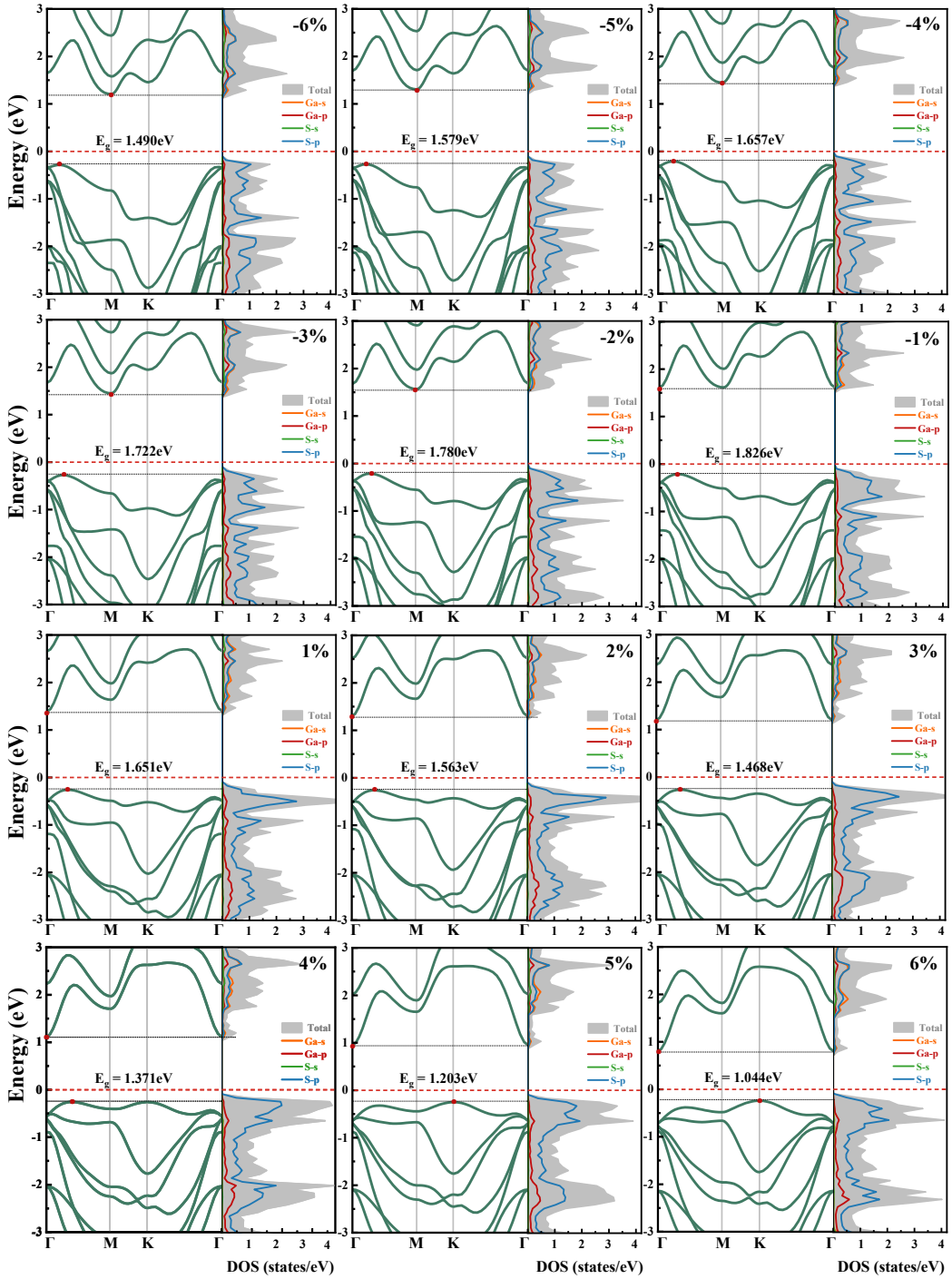

FIG. S5 Band structures and DOS of α-Ga_2S_3 under biaxial strain.

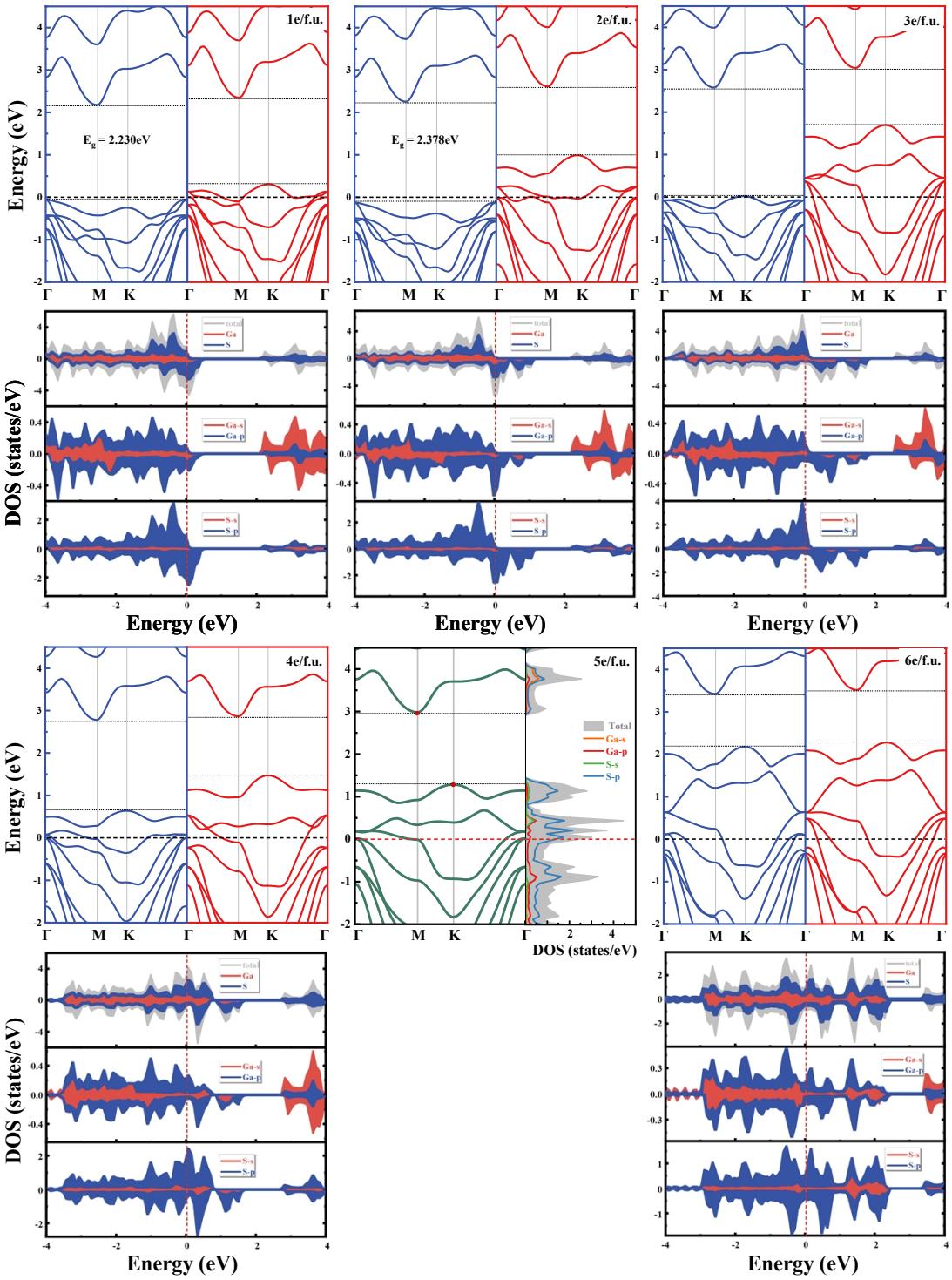

FIG. S6 Band Structures and DOS of α-Ga_2S_3 at the doping concentration of 1e/f.u. ~ 6e/f.u.

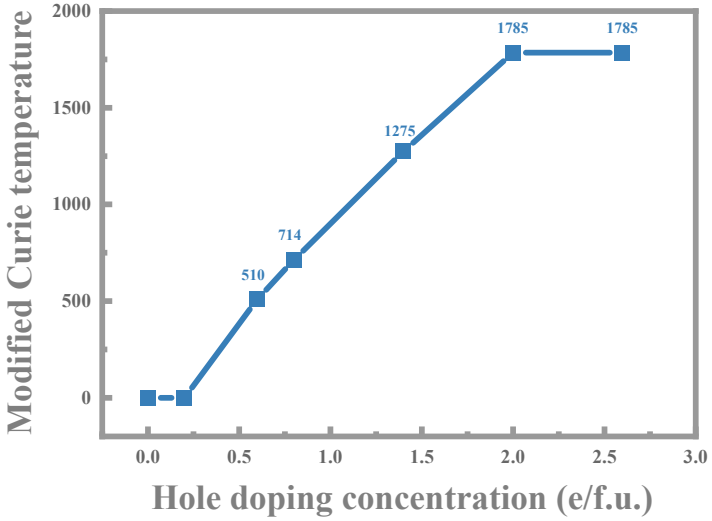

FIG. S7 The modified Curie temperature with hole-doping. Here, the modified T_C are calculated from the empirical relation ($T_C/T_C^{FM} = 0.51$, where the T_C^{FM} is the value obtained from the mean field method).

FIG. S8 Changes of out-of-plane spontaneous polarization and magnetic moment along the structures of ferroelectric switch path at the hole-doping concentration of 6 e/f.u. in pristine α-Ga_2S_3 monolayer.

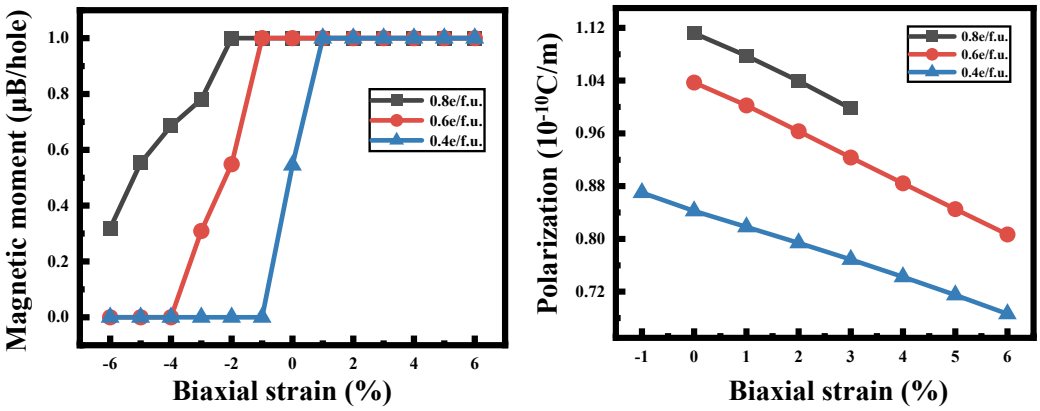

FIG. S9 Magnetic moment and $P_{out\text{-}of\text{-}plane}$ variation of different hole doping concentrations under biaxial strain.

Structures (readable by VASP)

POSCAR of FE phase

Ga S

1.0

3.6257998943000000 0.0000000000000000 0.0000000000000000

-1.8128999472000000 3.1400348175000001 0.0000000000000000

0.0000000000000000 0.0000000000000000 23.9799995422000016

Ga S

2 3

Direct

0.6666666870000000 0.3333333430000000 0.4261800050000000

0.3333333430000000 0.6666666870000000 0.5820400120000000

0.6666666870000000 0.3333333430000000 0.5186600090000000

0.0000000000000000 0.0000000000000000 0.6298400159999999

0.0000000000000000 0.0000000000000000 0.3819899860000000

CONTCAR of PE phase

Ga S

1.00000000000000

3.5347524519648537 0.0000000000000000 0.0000000000000000

-1.7667983159310483 3.0618323967901540 0.0000000000000000

-4.7867835502522516 2.8354013709060251 22.6445722957090005

Ga S

2 3

Direct

0.7639463216560429 0.2354848569522616 0.4252212230887196

0.2343825334817069 0.7663537199392678 0.5744004124108599

0.4992267664968750 0.5004949630778199 0.4998117570942995

0.9469904052064919 0.0520547136791265 0.6258872015620227

0.0513567037128837 0.9496991945127249 0.3737338988704053

CONTCAR of V_{Ga}

Ga S

1.00000000000000

10.8774003983000007 0.0000000000000000 0.0000000000000000

-5.4387001991000004 9.4201050720000001 0.0000000000000000

0.0000000000000000 0.0000000000000000 23.9799995422000016

Ga S

17 27

Direct

0.2273095009119601 0.1210639697125916 0.4240638131617041

0.1101402383383326 0.2217351221691684 0.5806758084526423

0.5604244638006378 0.1210639697125916 0.4240638131617041

0.4438506362837589 0.2210412625675238 0.5771213612242694

0.8888900279999987 0.1111100019999967 0.4235766632755147

0.7782648778308315 0.2217351221691684 0.5806758084526423

0.2273095009119601 0.4395755361993621 0.4240638131617041

0.1108384417249407 0.5550168724498913 0.5827983511089101

0.4438506362837589 0.5561493637162412 0.5771213612242694

0.8789360602874038 0.4395755361993621 0.4240638131617041

0.7789587374324761 0.5561493637162412 0.5771213612242694

0.2222200040000004 0.7777799959999996 0.4262048280239666

0.1108384417249407 0.8891615882750552 0.5827983511089101

0.5604244638006378 0.7726904990880399 0.4240638131617041

0.4449831275501092 0.8891615882750552 0.5827983511089101

0.8789360602874038 0.7726904990880399 0.4240638131617041

0.7782648778308315 0.8898597916616630 0.5806758084526423

0.2195577992323946 0.1082910915570775 0.5187852185644813

-0.0007205489378301 0.0007205489378301 0.6311610539100468

0.0008297614039787 -0.0008297614039787 0.3831656472094072

0.5554032873246895 0.1082910915570775 0.5187852185644813

0.3345236641121723 0.0023873182243437 0.6309485700575650

0.3333228298340168 -0.0000143503319673 0.3838768311215942

0.8888900279999987 0.1111100019999967 0.5180030064818831

0.6681111218756587 0.0007205489378301 0.6311610539100468

0.6650105011920411 -0.0008297614039787 0.3831656472094072

0.2195577992323946 0.4445967126753105 0.5187852185644813

-0.0007205489378301 0.3318889071243405 0.6311610539100468

0.0008297614039787 0.3349895278079579 0.3831656472094072

0.5555599930000028 0.4444400069999972 0.5182177844669846

0.3343883663965142 0.3338591856982575 0.6287696642946233

0.3483812590482098 0.3408556320241052 0.3878820461519274

0.8917089384429178 0.4445967126753105 0.5187852185644813

0.6661408433017417 0.3338591856982575 0.6287696642946233

0.6591443969758939 0.3408556320241052 0.3878820461519274

0.2222200040000004 0.7777799959999996 0.5200149808015513

-0.0023873182243437 0.6654763648878265 0.6309485700575650

0.0000143503319673 0.6666771991659821 0.3838768311215942

0.5554032873246895 0.7804422007676057 0.5187852185644813

0.3345236641121723 0.6654763648878265 0.6309485700575650

0.3333228298340168 0.6666771991659821 0.3838768311215942

0.8917089384429178 0.7804422007676057 0.5187852185644813

0.6661408433017417 0.6656116626034844 0.6287696642946233

0.6591443969758939 0.6516187699517890 0.3878820461519274

References:

1. L. Hu and X. Huang, *RSC Adv.*, 2017, **7**, 55034-55043.
2. G. Zhang, K. Lu, Y. Wang, H. Wang and Q. Chen, *Phys. Rev. B*, 2022, **105**, 235303.
3. R. Resta, M. Posternak and A. Baldereschi, *Phys. Rev. Lett.*, 1993, **70**, 1010.
4. D. Sheppard, P. Xiao, W. Chemelewski, D. D. Johnson and G. Henkelman, *J. Chem. Phys.*, 2012, **136**, 074103.
5. R. Fei, W. Kang and L. Yang, *Phys. Rev. Lett.*, 2016, **117**, 097601.
6. S. Zhang and J. E. Northrup, *Phys. Rev. Lett.*, 1991, **67**, 2339.
7. G. Baraff and M. Schlüter, *Phys. Rev. Lett.*, 1985, **55**, 1327.
8. J. He, K. Wu, R. Sa, Q. Li and Y. Wei, *Appl. Phys. Lett.*, 2010, **96**, 082504.
9. S.-H. Wei, *Comput. Mater. Sci.*, 2004, **30**, 337-348.
10. H. Chen, C.-Y. Wang, J.-T. Wang, X.-P. Hu and S.-X. Zhou, *J. Appl. Phys.*, 2012, **112**, 084513.
11. S.-H. Wei and S. Zhang, *Phys. Rev. B*, 2002, **66**, 155211.